Cooperative regulation of C1-domain membrane recruitment polarizes atypical Protein Kinase C

Kimberly A. Jones*, Michael L. Drummond*, and Kenneth E. Prehoda

Institute of Molecular Biology
Department of Chemistry and Biochemistry
1229 University of Oregon
Eugene, OR 97403

*Equal contributions

Corresponding author: prehoda@uoregon.edu

Abstract

Recruitment of the Par complex protein atypical Protein Kinase C (aPKC) to a specific membrane domain is a key step in the polarization of animal cells. While numerous proteins and phospholipids interact with aPKC, how these interactions cooperate to control its membrane recruitment has been unknown. Here we identify aPKC's C1 domain as a phospholipid interaction module that targets aPKC to the membrane of *Drosophila* neural stem cells (NSCs). The isolated C1 binds the NSC membrane in an unpolarized manner during interphase and mitosis and is uniquely sufficient among aPKC domains for targeting. Other domains, including the catalytic module and those that bind the upstream regulators Par-6 and Baz, restrict C1's membrane targeting activity spatially and temporally – to the apical NSC membrane during mitosis. Our results suggest that Par complex polarity results from cooperative activation of autoinhibited C1 membrane binding activity.

Introduction

The Par complex polarizes animal cells by excluding specific cortical factors from the Par cortical domain (Lang and Munro, 2017; Venkei and Yamashita, 2018). During polarization the Par complex, consisting of Par-6 and atypical Protein Kinase C (aPKC), is recruited to a specific, continuous region of the cell membrane such as the apical surface of epithelia (Tepass, 2012), the anterior hemisphere of the *C. elegans* zygote (Nance and Zallen, 2011), or the apical hemisphere of *Drosophila* neural stem cells (NSCs) (Prehoda, 2009). Factors that are polarized by the Par complex, such as Miranda and Numb, are aPKC substrates (Atwood and Prehoda, 2009; Smith et al., 2007). Phosphorylation is coupled to removal from the Par domain, causing these substrates to form a complementary membrane domain (Bailey and Prehoda, 2015). Thus, the pattern of Par-polarized factors is ultimately determined by the mechanisms that specify aPKC's membrane recruitment and activation.

Many aPKC interactions with proteins and phospholipids have been identified (Figure 1A), although how they collaborate to polarize aPKC remains poorly understood. Bazooka (Baz aka Par-3) and Par-6 form direct physical contacts with aPKC and each protein has possible pathways for membrane recruitment, Baz through direct interactions with the membrane and Par-6 through interactions with prenylated Cdc42 (Joberty et al., 2000; Lin et al., 2000; Krahn et al., 2010). Several direct interactions with phospholipids have also been reported, including with ceramide (Wang et al., 2005), sphingosine 1-phosphate (Kajimoto et al., 2019), and the phosphoinositides PI (4,5)P_2, and PI (3,4,5)-P_3 (Standaert et al., 1997). The aPKC catalytic

domain may also play a role in membrane recruitment as perturbations in this domain can cause aPKC to become depolarized (i.e. localized uniformly to the membrane) (Rodriguez et al., 2017; Hannaford et al., 2019).

While interactions that could potentially recruit aPKC to the membrane have been identified, what is missing is an understanding of how the interactions function together to yield aPKC polarity. One possibility is that each interaction is weak, unable to recruit aPKC to the membrane on its own, but the energy provided by multiple weak interactions allows for recruitment (i.e. avidity). Alternately, one or more interactions could be responsible for recruitment but somehow regulated to ensure that targeting only occurs when the appropriate cues are present. These models could be distinguished by determining if any interactions lead to constitutive membrane recruitment (i.e. if one or more domains were sufficient for targeting).

We used *Drosophila* NSCs to investigate how aPKC is recruited to the membrane during polarization (Homem and Knoblich, 2012). During NSC interphase, aPKC is cytoplasmic but becomes targeted to the apical hemisphere early in mitosis, ultimately concentrating near the apical pole before depolarizing and returning to the cytoplasm as division completes (Oon and Prehoda, 2019). The highly dynamic nature of the NSC polarity cycle makes it possible to assess both spatial (polarized, depolarized, or cytoplasmic) and temporal (interphase or mitotic) aspects of aPKC membrane recruitment regulation.

Results

Mutations that inactivate catalytic activity depolarize aPKC

We began our examination of aPKC membrane targeting mechanisms in NSCs by evaluating the role of the catalytic domain. At metaphase, aPKC is highly enriched at the apical membrane of larval brain NSCs (Rolls et al., 2003). We examined the effect of mutations that inactivate aPKC's catalytic activity on its localization in cells that lacked endogenous aPKC (*apkc*^{K06403} in positively marked clones; Lee and Luo, 1999). Besides aPKC's localization, we also examined its activity in these NSCs by determining the localization of Miranda (Mira), an aPKC substrate that is normally restricted to the basal cortex by apical aPKC activity (Figure 1B) (Atwood and Prehoda, 2009; Ikeshima-Kataoka et al., 1997). Consistent with previous observations, we found that in metaphase *apkc*^{K06403} NSCs, Mira was allowed to enter the apical cortex becoming uniformly cortical (Figure 1B). Furthermore, expression of wild-type

aPKC restored the apical aPKC and basal Mira localization found in normally functioning NSCs to *aPKC*^{K06403} null clones (Figure 1B, Holly et al., 2020).

To examine the effect of perturbing catalytic activity, we expressed aPKC harboring a mutation (D388A) that does not have detectable activity in an *in vitro* protein kinase assay (Holly et al., 2019). This mutation is in a residue that coordinates the γ-phosphate of ATP and is thought to prevent phosphotransfer while allowing ATP to bind (Cameron et al., 2009). Unlike wild-type aPKC, which is restricted to the apical domain at metaphase, we found that aPKC D388A was largely depolarized, localizing to the entire cortex of *aPKC*^{K06403} metaphase null clones (Figure 1A). Mira also localized uniformly to the cortex in these cells, confirming that aPKC D388A is inactive both *in vitro* (Holly et al., 2019) and *in vivo* (Figure 1B-F). Interestingly, the kinase inactivating mutation also caused aPKC to associate with the membrane during interphase, a cell cycle period in which it is normally cytoplasmic (Figure 1D,F). We conclude that inactivation of the aPKC catalytic domain causes aPKC to constitutively localize to the membrane.

Kinase inactive aPKC's localization is not restored by endogenous aPKC

Our results indicate that mutations that perturb aPKC's catalytic activity also influence its localization, both spatially and temporally, leading to constitutive depolarization. Previous observations using chemically inhibited aPKC also found that perturbations to catalytic activity caused depolarization (Rodriguez et al., 2017; Hannaford et al., 2019). The depolarization caused by perturbations to the kinase domain could be explained if aPKC's catalytic activity directly participated in its own localization (e.g. by activating an upstream regulator via phosphorylation). Alternately, however, perturbations in the kinase domain could alter other aPKC functions. Besides catalyzing phosphotransfer, the aPKC kinase domain also binds a pseudosubstrate in its NH_2-terminal region causing autoinhibition (Graybill et al., 2012). Mutations or small molecules that influence the active site could perturb the intramolecular interaction in addition to inhibiting catalytic activity. To determine whether the loss of aPKC's catalytic activity is responsible for the localization defects of D388A aPKC, we determined whether the presence of wild-type, endogenous aPKC with its normal level of catalytic activity could restore aPKC D388A polarity. We also tested the localization of a well-studied kinase inactive mutation K293W, which blocks ATP binding (Graybill et al, 2012). In NSCs containing endogenous aPKC, both aPKC D388A and K293W remained depolarized indicating that aPKC catalytic activity is not sufficient to restore polarity to these proteins. Interestingly, in cells expressing aPKC K293W Mira polarity was restored, confirming that aPKC activity was

present, but in cells expressing aPKC D388A, Mira remained depolarized suggesting that aPKC D388A influences the localization or activity of endogenous aPKC (Figure 1C).

We also examined whether kinase inactive aPKC mutants influence the localization of Baz or Par-6, proteins that directly interact with aPKC. We found that Baz remained apically polarized in cells expressing aPKC, as well as those expressing the aPKC D388A or aPKC K293W variants, although the intensity of this crescent was slightly reduced in aPKC D388A (Figure 2A, C). While Baz localization was unperturbed by the expression of the kinase inactive aPKC variants, Par-6 expanded into the basal domain like the localization of aPKC D388A and aPKC K293W (Figure 2A, B). This pattern of localization is similar to that of an analog sensitive variant of aPKC that also caused depolarization of Par-6 but not Baz (Hannaford et al., 2019). We conclude that expression of kinase inactive aPKC leads to loss of Par-6 polarity but does not influence the localization of Baz.

Kinase inactive aPKC binds the NSC membrane independent of Cdc42 and Bazooka

Membrane targeting of aPKC normally requires the activity of Baz and the small GTPase Cdc42 (Wodarz et al., 2000; Rolls et al., 2003; Atwood et al., 2007). We tested whether these upstream regulators are required for the uniformly cortical localization of kinase inactive aPKC by examining the localization of aPKC K293W in NSCs expressing Baz or Cdc42 RNAi. We found that wild-type aPKC failed to recruit to the membrane in these contexts, as previously reported (Figure 3A-D) (Atwood et al., 2007; Rolls et al., 2003). Consistent with this observation, we found that Mira was depolarized, localizing uniformly to the cortex in these cells. In contrast to wild-type aPKC, however, aPKC K293W was able to remain on the cortex even when Cdc42 was absent (Figure 3A-B). We also examined the localization of aPKC and the K293W variant in NSCs expressing Baz RNAi. In this context, wild-type aPKC appears more cytoplasmic and Mira becomes depolarized as expected (Atwood et al., 2007). Like NSCs expressing Cdc42 RNAi, however, aPKC K293W's cortical localization was not affected when Baz was reduced (Figure 3C-D). We conclude that aPKC K293W does not rely on Cdc42 or Baz for cortical targeting.

The aPKC C1 domain is a constitutive membrane targeting module

Our results indicate that the uniform membrane localization of aPKC with inactive kinase domains (e.g. K293W) is independent of both Baz and Cdc42. One model consistent with these results is that aPKC contains a membrane targeting module that is regulated by its

kinase domain, Baz, and Cdc42. To identify the putative module, we first examined whether removing the kinase domain leads to the same uniform membrane localization phenotype. As shown in Figure 4B, D-E, aPKC PB1-C1 (i.e. ΔKD) was uniformly localized in NSCs. A similar localization pattern has been reported for aPKC PB1-C1 expressed in cultured cells (Dong et al., 2020). Thus, aPKC's NH_2-terminal regulatory region contains the domain responsible for membrane binding. The regulatory region has three domains, PB1, PS and C1, each of which has the potential to interact with the membrane. The PB1 could mediate interaction with the membrane via protein-protein interactions with Par-6 (Atwood et al., 2007; Petronczki and Knoblich, 2001), the PS domain through direct interactions with lipids (Dong et al., 2020), and the C1 which serves as a membrane targeting module in other PKCs (Colón-González and Kazanietz, 2006), but has not been reported to do so in aPKCs. Removal of the C1 domain from the regulatory domain (aPKC PB1-PS) leaving the PB1 and PS domains, resulted in a protein that was not enriched at the membrane (Figure 4). Thus, the C1 domain is required for membrane localization of the regulatory region – the PB1 and PS domains are not sufficient for membrane targeting in NSCs. We next tested the C1 domain alone and found that it is sufficient for uniform targeting to the membrane (Figure 4B-D). During interphase the C1 domain was bound to membrane but also highly nuclear enriched (Figure 4C). Thus, the aPKC C1 domain is a membrane targeting module.

C1 is a lipid binding module that is required for aPKC membrane recruitment

How might the C1 domain mediate interaction with the NSC membrane? C1 domains in canonical PKCs bind diacylglycerol, and although the aPKC C1 domain does not bind DAG (Colón-González and Kazanietz, 2006), we sought to determine if it binds other phospholipids. We used a vesicle pelleting assay in which Giant Unilamellar Vesicles (GUVs) with varying phospholipid compositions were mixed with purified aPKC C1 domain. The vesicles were separated from the soluble phase by ultracentrifugation and any associated C1 was identified by protein gel electrophoresis. As shown in Figure 5A, we observed varying degrees of C1 binding to a broad array of phospholipids, suggesting that the C1 is a nonspecific phospholipid binding module.

To better understand the role of the C1 in aPKC polarity, we examined the effect of removing it (aPKC ΔC1) on aPKC's localization. As shown in Figure 4B-E, we found that aPKC ΔC1 remained in the cytoplasm, failing to bind the membrane. We conclude that the C1 is required for aPKC membrane targeting in NSCs. Interestingly, Mira localization was also disrupted in

158 NSCs expressing aPKC ΔC1 suggesting that the C1 also plays a role in regulating aPKC's
159 protein kinase activity in NSCs. This observation is consistent with *in vitro* measurements of
160 kinase activity (Graybill et al., 2012; Zhang et al., 2014).

161 The PS domain has been reported to be a membrane binding module required for membrane
162 recruitment of aPKC in cultured cells and epithelia (Dong et al., 2020). Our results suggest that
163 the PS is not sufficient for localization to the NSC membrane (e.g. aPKC PB1-PS remains in the
164 cytoplasm). We tested whether the PS is required for NSC aPKC membrane recruitment by
165 examining the localization of aPKC in which the positively charged, basic residues were
166 removed and a negative charge added (aPKC AADAA). This mutation has been reported to
167 abrogate membrane binding in contexts where the PS is required (Dong et al., 2020). We found
168 that the apical localization of aPKC AADAA was only slightly reduced compared to WT aPKC
169 indicating that the PS is not required for aPKC's membrane recruitment or polarization in NSCs
170 (Figure 5B-E). Mira was cytoplasmic in NSCs expressing aPKC AADAA, however, indicating
171 that disrupting the PS activates kinase activity, consistent with the known function of the PS in
172 regulating catalytic activity (Graybill et al., 2012).

173 **Discussion**

174 The Par complex component aPKC undergoes a complex localization cycle in NSCs, targeting
175 to the apical membrane in mitosis and returning to the cytoplasm as division completes (Oon
176 and Prehoda, 2019). The function of interphase, cytoplasmic localization is unknown, but the
177 apical localization of aPKC during mitosis is necessary for the polarization of fate determinants
178 (Atwood et al., 2007; Prehoda, 2009; Rolls et al., 2003), a prerequisite for asymmetric cell
179 division. Regulated membrane recruitment of aPKC is a central aspect of Par-mediated polarity
180 and many physical interactions between aPKC and proteins and phospholipids have been
181 identified. Conceptually, targeting could occur through the concerted action of multiple weak
182 interactions (i.e., avidity). However, we discovered that the aPKC C1 domain is a phospholipid
183 binding module sufficient for membrane recruitment, whereas domains that mediate protein-
184 protein interactions or other interactions with phospholipids are not sufficient for aPKC
185 targeting. As the C1 is the only domain within aPKC with this capability in NSCs, our results
186 suggest that other aPKC domains, including the catalytic domain, function, at least in part, to
187 regulate the membrane recruitment activity of the C1. We propose that cooperative activation
188 of the C1 leads to the spatially and temporally controlled localization of aPKC observed in
189 many animal cells.

The C1 is unique in its ability to promote aPKC membrane recruitment in NSCs. While numerous interactions between phospholipids and domains outside the C1 have been reported (Wang et al., 2005; Ivey et al., 2014; Kajimoto et al., 2019; Dong et al., 2020), our results indicate that they are not sufficient for membrane recruitment in NSCs. Similarly, the domains that mediate protein-protein interactions, such as the PB1 that binds Par-6 and the PBM that binds Baz, are also not sufficient for aPKC recruitment.

The constitutive nature of C1 membrane binding raises the question of how its activity is regulated to yield aPKC's precisely controlled localization. The aPKC catalytic domain forms intramolecular interactions with the PS and C1 that repress kinase activity (Graybill et al., 2012; Lopez-Garcia et al., 2011; Zhang et al., 2014), forming an "inhibitory core" (Figure 5F). Our results suggest the inhibitory core is coupled to C1 membrane binding. We observed C1 localization at the membrane throughout the cell cycle and uniform membrane binding in mitosis when aPKC is normally restricted to the apical hemisphere. We also observed constitutive membrane recruitment in aPKC variants where the catalytic domain was perturbed, suggesting that it is required for repression of C1 activity. We suggest that perturbations to the catalytic domain that influence protein kinase activity can also disrupt the inhibitory core, consistent with the complex allosteric pathways in eukaryotic protein kinase domains (Ahuja et al., 2019). It has been proposed that the PS plays a central role in membrane recruitment and coupling localization to the inhibitory core through its interactions with the catalytic domain (Dong et al., 2020). Our results indicate that the PS is not sufficient for membrane recruitment, nor is its interaction with the aPKC catalytic domain required for polarization in NSCs (aPKC AADAA is polarized but constitutively active). We conclude that, at least in NSCs, the PS plays a more significant role in regulating catalytic activity than localization.

Given that the C1 appears to be autoinhibited by the catalytic domain, how might it become activated? We previously found that inactivation of the aPKC PBM (aPKC V606A), which binds Baz, leads to cytoplasmic aPKC localization (Holly et al., 2020). Taken with our current results, we suggest that the interaction with Baz is required for membrane recruitment not because Baz directly recruits aPKC (e.g. aPKC ΔC1 is cytoplasmic), but because the Baz interaction is required for disruption of the inhibitory core and activation of the C1. Similarly, in NSCs lacking the PB1-binding Par-6 protein, aPKC also remains in the cytoplasm, even though Baz remains properly polarized and could potentially bind aPKC's PBM. We propose that cooperative

activation of the C1 by at least Par-6 and Baz leads to the complex localization dynamics of aPKC observed in NSCs. Future work will be directed at understanding how the aPKC PB1 and PBM might be coupled to the inhibitory core and activation of aPKC membrane binding.

Materials and Methods

Drosophila

Flies were grown at indicated temperatures on standard cornmeal/yeast media. Both male and female larvae were used in this study. Transgenic constructs were cloned into the pUAST attB vector (GenBank: EF362409.1) modified to include an N-terminal 3xHA or 1xHA tag. Integration of the vectors was done using standard Phi-C31 integration into an attP landing site on the third chromosome (attP2) by Rainbow Genetics or BestGene Inc. Positive insertion was determined by the presence of colored eyes after backcrossing to y,w stock.

Immunofluorescence

For all overexpression crosses, *insc*-Gal4 virgins were crossed to males containing an aPKC transgene on the third chromosome or an RNAi on the second chromosome and an aPKC transgene on the third chromosome. Crosses laid in vials for 24 hours (~20˚C) for 24 hours. The resulting embryos were incubated at 30˚C until larvae reached third instar wandering larva stage. Following dissection, the tissue was incubated in 4% PFA fixative for 20’ within 20’ of dissection. This and all subsequent wash steps involved agitation by placing on a nutator. After fixation, brains were washed 1xquick, and 3x15’ in PBST (1xPBS with 0.3% Triton-X). If brains were not to be stained that day, they would then be placed at 4˚C for up to 3 days after which a quick wash in PBST would be required before moving on to staining. If instead they were to be stained, an additional wash step of 20’ in PBST would occur. Brains were blocked for 30’ in PBSBT (PBST with 1% BSA) and then put into 1˚ overnight at 4˚C. The next day after removing the 1˚, brains were washed 1xquick and 3x15’ in PBSBT and put into 2˚ for 2 hours, protected from light. After 2˚ was removed, brains were washed 1xquick and 3x15’ in PBST. Brains were stored in SlowFade w/DAPI at least overnight before imaging. Brains were imaged on an upright confocal TCS SPE from Leica using an ACS APO 40x 1.15 NA Oil CS objective.

MARCM Immunofluorescence

To create MARCM larval NSC clones, FRT-G13, aPKC^{K06403}/CyO virgins were crossed with 3xHA aPKC D388A males. The subsequent progeny were allowed to grow to adulthood and

were screened for the absence of the CyO marker. Males with no CyO were then crossed to elav-Gal4, UAS-mCD8:GFP, hs:flp; FRT-G13, tubPGal80 virgins.
Crosses laid in vials for 24 hours and the resulting embryos were incubated at room temperature (~20˚C) for 24 hours. These vials were then heat shocked at 37˚C for 90 min. Another heat shock was possible within 18 hours. Larvae were allowed to grow at room temperature or 18˚C until third instar wandering larva stage, when they were dissected and fixed as above.

Membrane enrichment and polarization quantification

Took measure of a 10px line through the central slice of a neuroblast from apical to basal cortex. Apical was taken as the peak corresponding with the apical membrane and basal was taken as the peak corresponding with the basal membrane. Where no peak was present, peaks in other channels or the “edge” of signal before it dropped was used. Cytoplasmic signal was taken as the average of 20 data points located 10 points from the apical peak.
All images were analyzed using Fiji and statistical analysis was done in Prizm.
All figures were put together using Adobe Illustrator.

Lipid pulldown assay

MBP-C1 was purified according to standard MBP purification protocols in our lab as previously described (Graybill et al., 2012). For Giant Unilamellar Vesical (GUV) production, 50 µl of the specified lipids at 10mg/mL in chloroform was dried in a test tube under an N_2 stream and then in a vacuum chamber to ensure all chloroform was removed. Lipids were resuspended in a 0.2M sucrose solution to a final concentration of 0.5mg/mL and heated in a water bath at 50˚C for 5 hours with occasional agitation. All lipids were stored at 4˚C and used within 3 days. For this assay, 10X Dilution Buffer was made: 200mM HEPES, pH 7.5; 500mM NaCl, 10mM DTT. All spins were carried out using an Optima MAX-TL Ultracentrifuge with a TLA-100 rotor at 65,000 at 4˚C.
MBP-C1 protein was diluted to 50µM in 1xDilution Buffer and pre-cleared for 30’. Reaction conditions: 20mM HEPES, pH 7.5, 50mM NaCl, 1mM DTT, 0.25mg/mL GUVs, and 5µM MBP-C1. Reaction was carried out at room temperature for 15’ and then spun down for 30’. The supernatant fraction was removed, and the pellet was resuspended in an equivalent volume of 1X Dilution buffer. Both the supernatant and pellet samples were mixed with 6x loading dye

and run on a 12.5% SDS-Page gel. Gels were stained with Coomassie and imaged using a scanner.

Key Resources Table

Reagent type (species) or resource	Designation	Source or reference	Identifiers	Additional information
antibody	anti-aPKC	SCBT	Mouse Anti-PKC zeta (H1); SC-17781	1:1000
antibody	anti-Par-6	Alpha diagnostic	N/A	Rat Anti-Par-6 (polyclonal custom antibody); 1:500
antibody	anti-Mira	Abcam	Rat Anti-Mira; Ab197788	1:500
antibody	anti-HA	Cell Signaling Tech.	Rabbit Anti-HA (C29F4); 3724	1:1000
antibody	anti-HA	Covance	Mouse Anti-HA; MMS-101P	1:500
antibody	anti-Baz	C.Q.Doe Lab	N/A	Guinea Pig Anti-Baz (polyclonal custom antibody); 1:2000
antibody	anti-GFP	Abcam	Chicken Anti-GFP; Ab13970	1:500
antibody	anti-rat Cy3 secondary	Jackson Immuoresearch Lab.	Donkey Anti-Rat Cy3; 712-165-153	1:500
antibody	anti-rabbit 647 secondary	Jackson Immunoresearch Lab.	Donkey Anti-Rabbit 647; 711-605-152	1:500
antibody	anti-mouse 647 secondary	Jackson Immunoresearch Lab.	Donkey Anti-Mouse 647; 715-605-151	1:500
antibody	anti-mouse 488 secondary	Jackson Immunoresearch Lab.	Donkey Anti-Mouse 488; 715-545-151	1:500
antibody	anti-chicken 488 secondary	Jackson Immunoresearch Lab.	Donkey Anti-Chicken 488; 703-545-155	1:500
antibody	anti-guinea pig 405 secondary	Jackson Immunoresearch Lab.	Donkey Anti-Guinea Pig 405; 706-475-148	1:500
genetic reagent (*Drosophila melanogaster*)	*insc-GAL4*	Bloomington Drosophila Stock Center	*;insc-GAL4*	RRID:BDSC_8751

genetic reagent (*Drosophila melanogaster*)	*elav-GAL4*	Bloomington Drosophila Stock Center	*elav-Gal4, UAS-mCD8:GFP, hs:flp; FRT-G13, tubPGal80*	RRID:BDSC_5145
genetic reagent (*Drosophila melanogaster*)	*aPKC^{K06403}*	C.Q. Doe Lab	*; FRT-G13, aPKCK^{06403}/CyO*	
genetic reagent (*Drosophila melanogaster*)	HA-aPKC D388A	This study	;;3xHA-aPKC D388A (aPKC-PA)	
genetic reagent (*Drosophila melanogaster*)	HA-aPKC D388A	This study	;;1xHA-aPKC D388A (aPKC-PA)	
genetic reagent (*Drosophila melanogaster*)	HA-aPKC	This study	;;1xHA-aPKC 1-606 (aPKC-PA)	
genetic reagent (*Drosophila melanogaster*)	aPKC K293W	This study	;;1xHA-aPKC K293W (aPKC-PA)	
genetic reagent (*Drosophila melanogaster*)	aPKC PB1-C1	This study	;;1xHA-aPKC 1-195 (aPKC-PA)	
genetic reagent (*Drosophila melanogaster*)	aPKC PB1-PS	This study	;;1xHA-aPKC 1-141 (aPKC-PA)	
genetic reagent (*Drosophila melanogaster*)	aPKC C1	This study	;;1xHA-aPKC 139-195 (aPKC-PA)	
genetic reagent (*Drosophila melanogaster*)	aPKC ΔC1	This study	;;1xHA-aPKC 1-606 Δ141-196 (aPKC-PA)	
genetic reagent (*Drosophila melanogaster*)	aPKC AADAA	This study	;;1xHA-aPKC R131A, R132A, A134D, R135A, R136A (aPKC-PA)	
genetic reagent (*Drosophila melanogaster*)	Baz RNAi	Bloomington Drosophila Stock Center	*;UAS-Baz RNAi*	RRID:BDSC_39072
genetic reagent (*Drosophila melanogaster*)	Cdc42 RNAi	Bloomington Drosophila Stock Center	*;UAS-Cdc42 RNAi*	RRID:VDRC_100794
chemical compound, drug	Amylose Resin	NEB	E8021L	
chemical compound, drug	Schneider's Insect Medium (SIM)	Sigma	S0146	
chemical compound, drug	SlowFade Diamond Antifade Mountant with DAPI	Invitrogen	S36964	

chemical compound, drug	Phosphatidylserine (PS)	Avanti Polar Lipids	L-α-phosphatidylserine; 840032C	
chemical compound, drug	Phosphatidylcholine (PC)	Avanti Polar Lipids	L-α-phosphatidylcholine; 840051C	
chemical compound, drug	Phosphatidic acid (PA)	Avanti Polar Lipids	L-α-phosphatidic acid; 840101C	
chemical compound, drug	Phosphatidylglycerol (PG)	Avanti Polar Lipids	L-α-phosphatidylglycerol; 841138P	
chemical compound, drug	ceramide	Avanti Polar Lipids	C12 ceramide; 860512P	

References

Ahuja LG, Taylor SS, Kornev AP. 2019. Tuning the "violin" of protein kinases: The role of dynamics-based allostery. *IUBMB Life* **71**:685–696. doi:10.1002/iub.2057

Atwood SX, Chabu C, Penkert RR, Doe CQ, Prehoda KE. 2007. Cdc42 acts downstream of Bazooka to regulate neuroblast polarity through Par-6 aPKC. *J Cell Sci* **120**:3200–3206. doi:10.1242/jcs.014902

Atwood SX, Prehoda KE. 2009. aPKC phosphorylates Miranda to polarize fate determinants during neuroblast asymmetric cell division. *Curr Biol CB* **19**:723–729. doi:10.1016/j.cub.2009.03.056

Bailey MJ, Prehoda KE. 2015. Establishment of Par-Polarized Cortical Domains via Phosphoregulated Membrane Motifs. *Dev Cell* **35**:199–210. doi:10.1016/j.devcel.2015.09.016

Colón-González F, Kazanietz MG. 2006. C1 domains exposed: from diacylglycerol binding to protein-protein interactions. *Biochim Biophys Acta* **1761**:827–837. doi:10.1016/j.bbalip.2006.05.001

Dong W, Lu J, Zhang X, Wu Y, Lettieri K, Hammond GR, Hong Y. 2020. A polybasic domain in aPKC mediates Par6-dependent control of membrane targeting and kinase activity. *J Cell Biol* **219**:e201903031. doi:10.1083/jcb.201903031

Graybill C, Wee B, Atwood SX, Prehoda KE. 2012. Partitioning-defective protein 6 (Par-6) activates atypical protein kinase C (aPKC) by pseudosubstrate displacement. *J Biol Chem* **287**:21003–21011. doi:10.1074/jbc.M112.360495

Hannaford M, Loyer N, Tonelli F, Zoltner M, Januschke J. 2019. A chemical-genetics approach to study the role of atypical Protein Kinase C in Drosophila. *Dev Camb Engl* **146**:dev170589. doi:10.1242/dev.170589

Holly RW, Jones K, Prehoda KE. 2020. A Conserved PDZ-Binding Motif in aPKC Interacts with Par-3 and Mediates Cortical Polarity. *Curr Biol CB* **30**:893-898.e5. doi:10.1016/j.cub.2019.12.055

Homem CCF, Knoblich JA. 2012. Drosophila neuroblasts: a model for stem cell biology **139**:4297–4310. doi:10.1242/dev.080515

Ikeshima-Kataoka H, Skeath JB, Nabeshima Y, Doe CQ, Matsuzaki F. 1997. Miranda directs Prospero to a daughter cell during Drosophila asymmetric divisions. *Nature* **390**:625–629. doi:10.1038/37641

Ivey RA, Sajan MP, Farese RV. 2014. Requirements for pseudosubstrate arginine residues during autoinhibition and phosphatidylinositol 3,4,5-$(PO_4)_3$-dependent activation of atypical PKC. *J Biol Chem* **289**:25021–25030. doi:10.1074/jbc.M114.565671

Joberty G, Petersen C, Gao L, Macara IG. 2000. The cell-polarity protein Par6 links Par3 and atypical protein kinase C to Cdc42. *Nat Cell Biol* **2**:531–539. doi:10.1038/35019573

Kajimoto T, Caliman AD, Tobias IS, Okada T, Pilo CA, Van A-AN, Andrew McCammon J, Nakamura S-I, Newton AC. 2019. Activation of atypical protein kinase C by sphingosine 1-phosphate revealed by an aPKC-specific activity reporter. *Sci Signal* **12**:eaat6662. doi:10.1126/scisignal.aat6662

Krahn MP, Klopfenstein DR, Fischer N, Wodarz A. 2010. Membrane targeting of Bazooka/PAR-3 is mediated by direct binding to phosphoinositide lipids. *Curr Biol CB* **20**:636–642. doi:10.1016/j.cub.2010.01.065

Lang CF, Munro E. 2017. The PAR proteins: from molecular circuits to dynamic self-stabilizing cell polarity. *Dev Camb Engl* **144**:3405–3416. doi:10.1242/dev.139063

Lin D, Edwards AS, Fawcett JP, Mbamalu G, Scott JD, Pawson T. 2000. A mammalian PAR-3-PAR-6 complex implicated in Cdc42/Rac1 and aPKC signalling and cell polarity. *Nat Cell Biol* **2**:540–547. doi:10.1038/35019582

Lopez-Garcia LA, Schulze JO, Fröhner W, Zhang H, Süss E, Weber N, Navratil J, Amon S, Hindie V, Zeuzem S, Jørgensen TJD, Alzari PM, Neimanis S, Engel M, Biondi RM. 2011. Allosteric regulation of protein kinase PKCζ by the N-terminal C1 domain and small compounds to the PIF-pocket. *Chem Biol* **18**:1463–1473. doi:10.1016/j.chembiol.2011.08.010

Nance J, Zallen JA. 2011. Elaborating polarity: PAR proteins and the cytoskeleton. *Dev Camb Engl* **138**:799–809. doi:10.1242/dev.053538

Oon CH, Prehoda KE. 2019. Asymmetric recruitment and actin-dependent cortical flows drive the neuroblast polarity cycle. *eLife* **8**. doi:10.7554/eLife.45815

Petronczki M, Knoblich JA. 2001. DmPAR-6 directs epithelial polarity and asymmetric cell division of neuroblasts in Drosophila. *Nat Cell Biol* **3**:43–49. doi:10.1038/35050550

Prehoda KE. 2009. Polarization of Drosophila neuroblasts during asymmetric division. *Cold Spring Harb Perspect Biol* **1**:a001388. doi:10.1101/cshperspect.a001388

Rodriguez J, Peglion F, Martin J, Hubatsch L, Reich J, Hirani N, Gubieda AG, Roffey J, Fernandes AR, St Johnston D, Ahringer J, Goehring NW. 2017. aPKC Cycles between Functionally Distinct PAR Protein Assemblies to Drive Cell Polarity. *Dev Cell* **42**:400-415.e9. doi:10.1016/j.devcel.2017.07.007

Rolls MM, Albertson R, Shih H-P, Lee C-Y, Doe CQ. 2003. Drosophila aPKC regulates cell polarity and cell proliferation in neuroblasts and epithelia. *J Cell Biol* **163**:1089–1098. doi:10.1083/jcb.200306079

Smith CA, Lau KM, Rahmani Z, Dho SE, Brothers G, She YM, Berry DM, Bonneil E, Thibault P, Schweisguth F, Le Borgne R, McGlade CJ. 2007. aPKC-mediated phosphorylation regulates asymmetric membrane localization of the cell fate determinant Numb. *EMBO J* **26**:468–480. doi:10.1038/sj.emboj.7601495

Standaert ML, Galloway L, Karnam P, Bandyopadhyay G, Moscat J, Farese RV. 1997. Protein kinase C-zeta as a downstream effector of phosphatidylinositol 3-kinase during insulin stimulation in rat adipocytes. Potential role in glucose transport **272**:30075–30082.

Tepass U. 2012. The Apical Polarity Protein Network in Drosophila Epithelial Cells: Regulation of Polarity, Junctions, Morphogenesis, Cell Growth, and Survival **28**:655–685. doi:10.1146/annurev-cellbio-092910-154033

Venkei ZG, Yamashita YM. 2018. Emerging mechanisms of asymmetric stem cell division. *J Cell Biol*. doi:10.1083/jcb.201807037

Wang G, Silva J, Krishnamurthy K, Tran E, Condie BG, Bieberich E. 2005. Direct binding to ceramide activates protein kinase Czeta before the formation of a pro-apoptotic complex with PAR-4 in differentiating stem cells. *J Biol Chem* **280**:26415–26424. doi:10.1074/jbc.M501492200

Wodarz A, Ramrath A, Grimm A, Knust E. 2000. Drosophila atypical protein kinase C associates with Bazooka and controls polarity of epithelia and neuroblasts. *J Cell Biol* **150**:1361–1374. doi:10.1083/jcb.150.6.1361

Zhang H, Neimanis S, Lopez-Garcia LA, Arencibia JM, Amon S, Stroba A, Zeuzem S, Proschak E, Stark H, Bauer AF, Busschots K, Jørgensen TJD, Engel M, Schulze JO, Biondi RM. 2014. Molecular mechanism of regulation of the atypical protein kinase C by N-terminal domains and an allosteric small compound. *Chem Biol* **21**:754–765. doi:10.1016/j.chembiol.2014.04.007

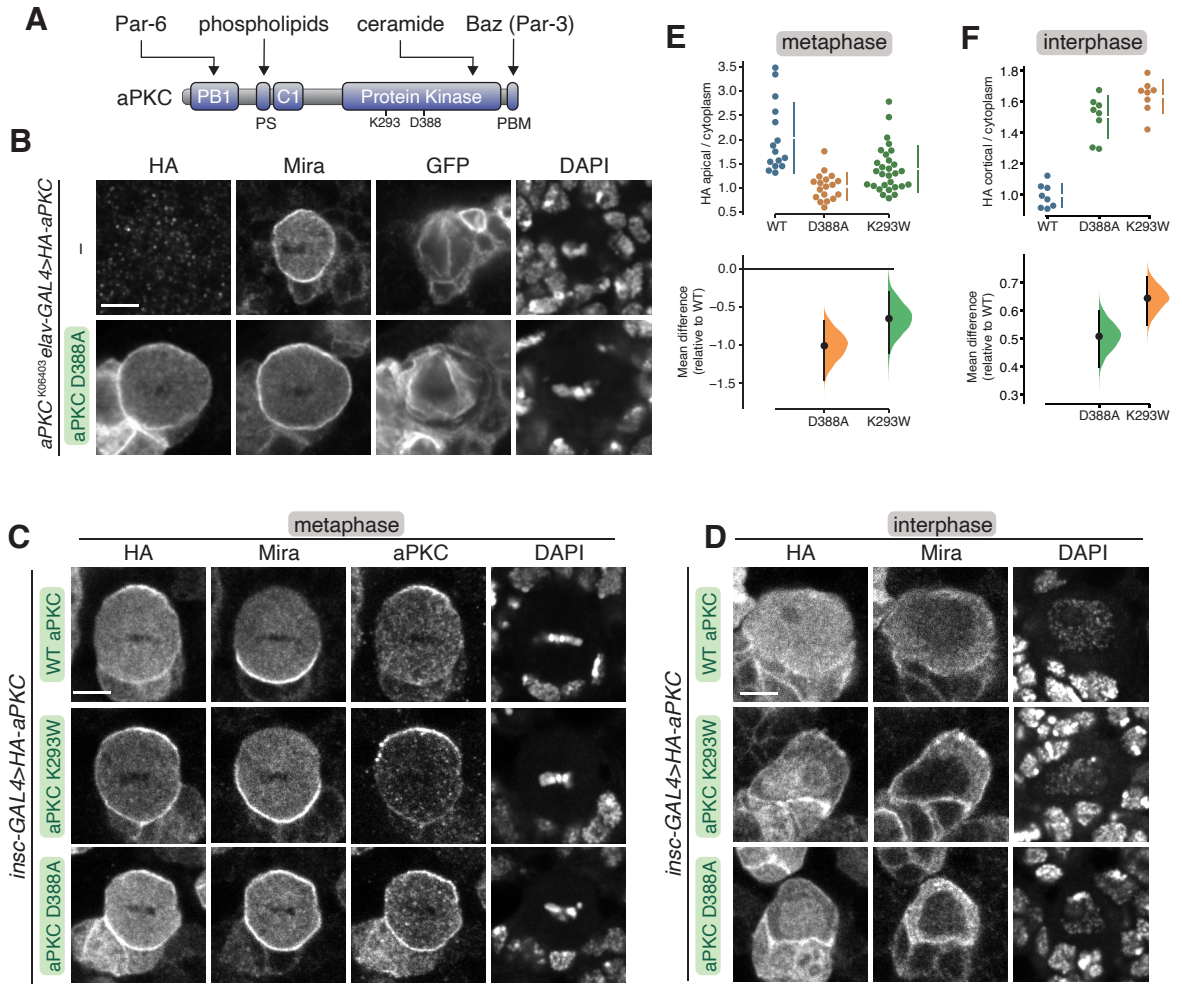

Figure 1 Localization of aPKC with kinase inactivating mutations in larval brain NSCs

(A) Domain structure of aPKC showing the location of PB1, PS (pseudosubstrate), C1, kinase domains, PBM (PDZ binding motif), along with location of K293 and D388 residues.

(B) Localization of HA tagged aPKC harboring the D388A kinase inactivating mutation in a metaphase, positively marked (mCD8-GFP) *aPKC*^{K06403} mutant larval brain NSC. Expression of D388A was driven by UAS and elav-GAL4. An *aPKC*^{K06403} mutant larval brain NSC is shown for comparison. Nucleic acids are shown with DAPI. Scale bar is 5 μm in all panels.

(C) Localization of HA tagged aPKC harboring either the D388A or K293W kinase inactivation mutations in metaphase larval brain NSCs with endogenous aPKC. The basal cortical marker Miranda, total aPKC ("aPKC", endogenous and exogenously expressed), and nucleic acid (DAPI) are also shown.

(D) Localization of HA tagged aPKC harboring either the D388A or K293W kinase inactivation mutations in interphase larval brain NSCs with endogenous aPKC. The basal cortical marker Miranda and nucleic acid (DAPI) are also shown.

(E) Gardner-Altman estimation plot of the effect of the D388A and K293W mutations on metaphase aPKC membrane recruitment. Apical cortical to cytoplasmic signal intensities of anti-HA signals are shown for individual metaphase NSCs expressing either HA-WT or HA-D388A or HA-K293W aPKC. Statistics: bootstrap 95% confidence interval (bar in “D388A” and “K293W” column).

(F) Gardner-Altman estimation plot of the effect of the D388A and K293W mutations on interphase aPKC membrane recruitment. Cortical to cytoplasmic cortical signal intensities of anti-HA signals are shown for individual metaphase NSCs expressing either HA-WT or HA-D388A or HA-K293W aPKC. Statistics: bootstrap 95% confidence interval (bar in “D388A” and “K293W” column).

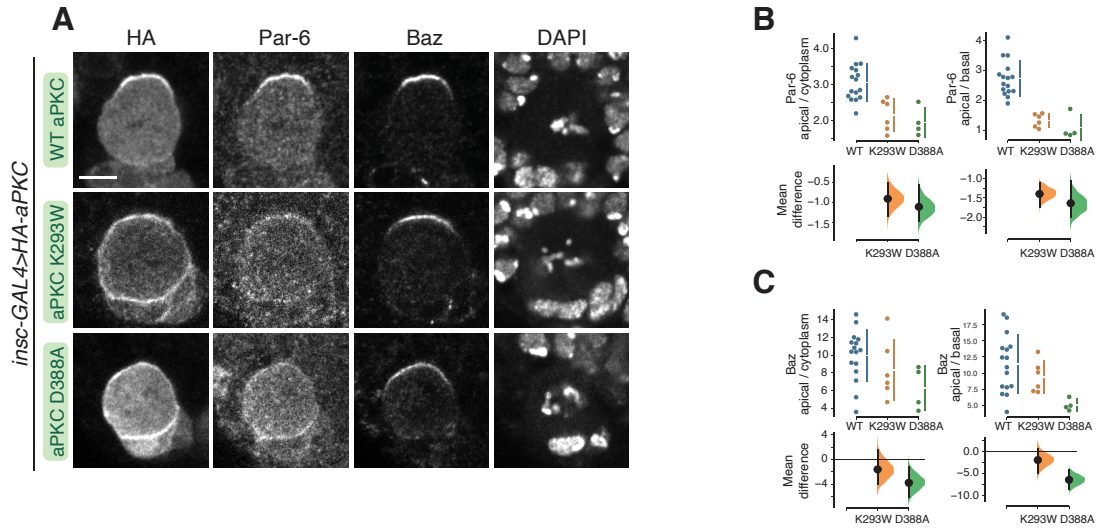

Figure 2 Localization of Bazooka and Par-6 in larval brain NSCs expressing kinase inactive aPKCs
(A) Localization of Par-6 and Bazooka (Baz) in metaphase larval brain NSCs expressing HA tagged aPKC D388A or aPKC K293W via UAS and insc-GAL4. Nucleic acids are shown with DAPI. Scale bar is 5 μm.
(B) Gardner-Altman estimation plots of the effect of expressing aPKC D388A or aPKC K293W on Par-6 cortical localization and polarity. Apical cortical to cytoplasmic or basal cortical signal intensities of anti-Par-6 signals are shown for individual metaphase NSCs expressing either HA-WT or HA-D388A or HA-K293W aPKC. Statistics: bootstrap 95% confidence interval (bar in "D388A" and "K293W" column).
(C) Gardner-Altman estimation plots of the effect of expressing aPKC D388A or aPKC K293W on Baz cortical localization and polarity. Apical cortical to cytoplasmic or basal cortical signal intensities of anti-Baz signals are shown for individual metaphase NSCs expressing either HA-WT or HA-D388A or HA-K293W aPKC. Statistics: bootstrap 95% confidence interval (bar in "D388A" and "K293W" column).

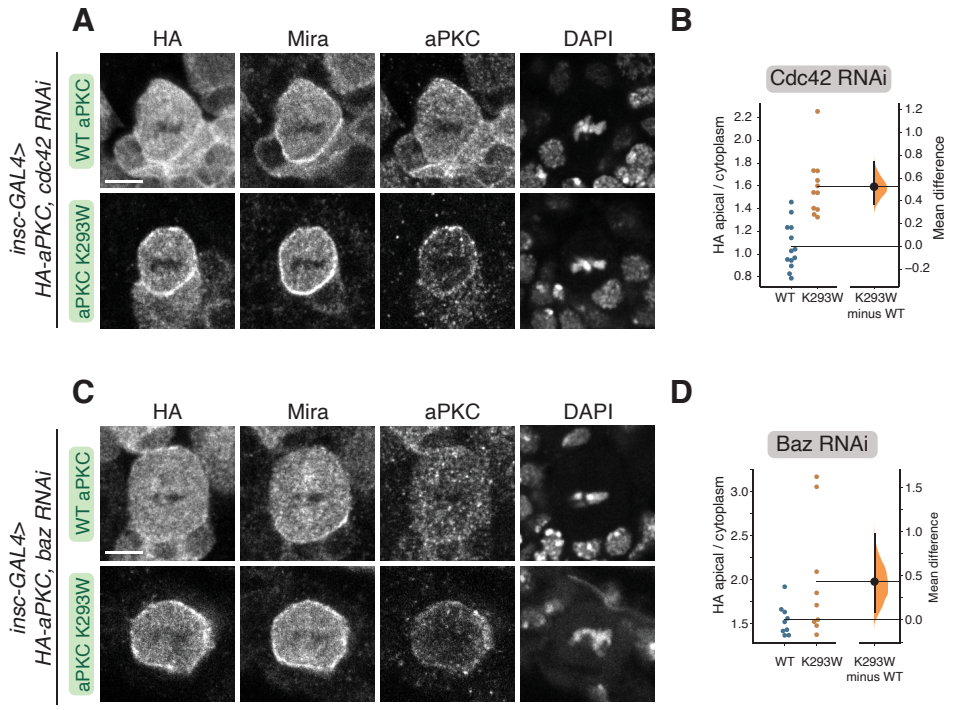

Figure 3 Cortical localization of kinase inactive aPKC in NSCs lacking Bazooka or Cdc42
(A) Localization of HA tagged aPKC K293W in metaphase larval brain NSCs expressing an RNAi directed against Cdc42. Scale bar is 5 μm in all panels.
(B) Gardner-Altman estimation plots of the effect of expressing Cdc42 RNAi on WT and K293W aPKC cortical localization. Apical cortical to cytoplasmic signal intensities of anti-HA signals are shown for individual metaphase NSCs expressing either HA-WT or HA-K293W aPKC. Statistics: bootstrap 95% confidence interval.
(C) Localization of HA tagged aPKC K293W in metaphase larval brain NSCs expressing an RNAi directed against Bazooka.
(D) Gardner-Altman estimation plots of the effect of expressing Baz RNAi on WT and K293W aPKC cortical localization. Apical cortical to cytoplasmic signal intensities of anti-HA signals are shown for individual metaphase NSCs expressing either HA-WT or HA-K293W aPKC. Statistics: bootstrap 95% confidence interval.

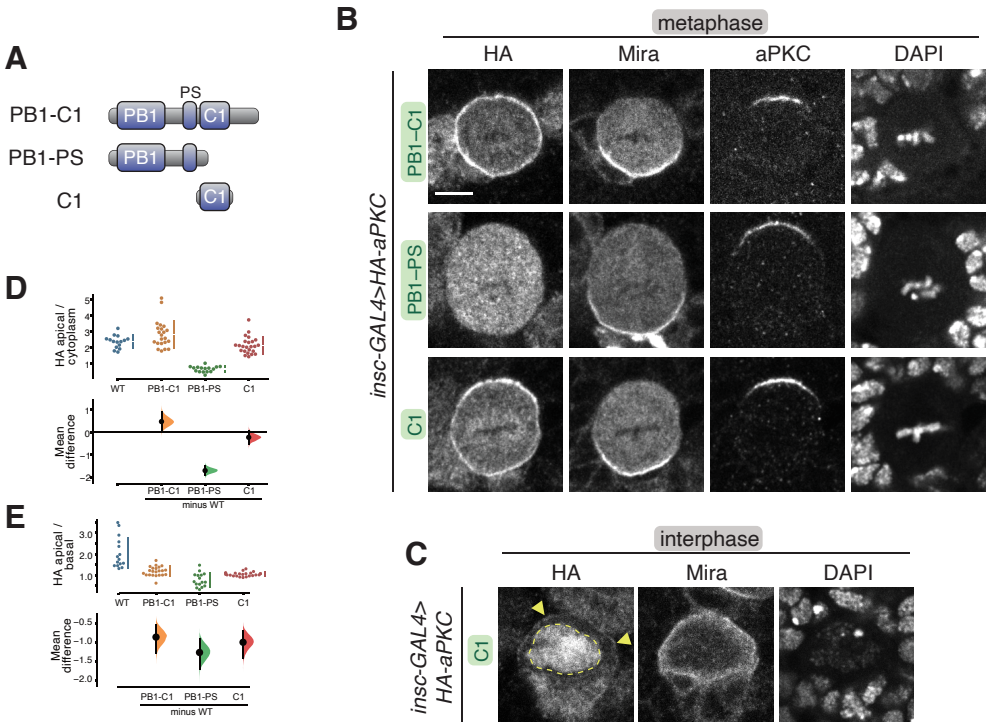

Figure 4 Localization of the aPKC regulatory domain variants in larval brain NSCs
(A) Schematics of regulatory domain variants of aPKC.
(B) Localization of HA tagged aPKC regulatory domain variants in metaphase larval brain NSCs. The basal marker Miranda, endogenous aPKC (using an antibody that does not react with the regulatory domain), nucleic acids (DAPI) are shown for comparison. Scale bar is 5 μm.
(C) Localization of the HA tagged aPKC C1 domain in interphase larval brain NSCs. Arrowheads highlight the membrane signal and the nuclear signal is outlined by a dashed line.
(D) Gardner-Altman estimation plot of aPKC regulatory domain cortical localization. Apical cortical to cytoplasmic signal intensity ratios of anti-HA signals are shown for individual metaphase NSCs expressing either aPKC PB1-C1 or PB1-PS or C1 regulatory domain fragments. Statistics: bootstrap 95% confidence interval.
(E) Gardner-Altman estimation plot of aPKC regulatory domain polarity. Apical cortical to basal cortical signal intensity ratios of anti-HA signals are shown for individual metaphase NSCs expressing either aPKC PB1-C1 or PB1-PS or C1 regulatory domain fragments. Statistics: bootstrap 95% confidence interval.

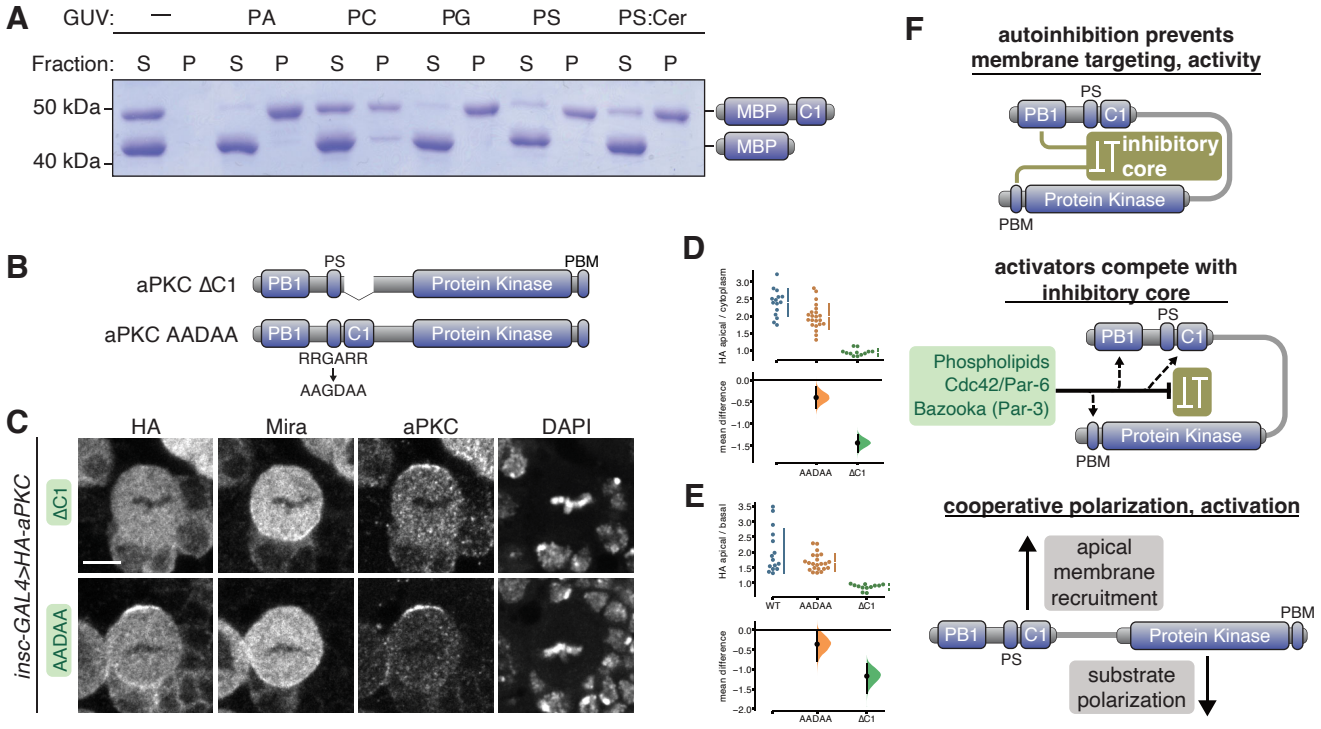

Figure 5 The aPKC C1 domain is a cortical localization module that is required for aPKC polarity
(A) Binding of a maltose binding protein (MBP) fusion of the aPKC C1 domain to phospholipids. Supernatant (S) and pellet (P) fractions from cosedimentation with Giant Unilamellar Vesicles (GUVs) of the indicated phospholipid composition are shown (PA, phosphatidic acid; PC, phosphatidyl choline; PG, phosphatidyl glycerol; PS, phosphatidyl serine; PS:Cer, phosphatidyl serine mixture with ceramide). MBP alone is included as an internal negative control.
(B) Schematics of ΔC1 and AADAA aPKC variants.
(C) Localization of HA tagged aPKC ΔC1 and AADAA variants in metaphase larval brain NSCs. The basal marker Miranda, total aPKC (expressed variant and endogenous), nucleic acids (DAPI) are shown for comparison. Scale bar is 5 μm.
(D) Gardner-Altman estimation plot of aPKC AADAA and ΔC1 cortical localization. Apical cortical to cytoplasmic signal intensity ratios of anti-HA signals are shown for individual metaphase NSCs expressing either aPKC AADAA or ΔC1. Statistics: bootstrap 95% confidence interval.
(E) Gardner-Altman estimation plot of aPKC AADAA and ΔC1 polarization. Apical cortical to basal cortical signal intensity ratios of anti-HA signals are shown for individual metaphase NSCs expressing either aPKC AADAA or ΔC1. Statistics: bootstrap 95% confidence interval.
(F) Model for cooperative polarization and activation of aPKC. An inhibitory core couples repression of catalytic activity (protein kinase domain) to membrane localization (C1 with some contribtion from PS). The PB1 and PBM are also coupled to the inhibitory core to allow for cooperative activation by Cdc42/Par-6 binding to the PB1 and Baz binding to the PBM. Disruption of the inhibitory core leads to spatially (apical) and temporally (mitotic) regulated localization and activation of catalytic activity.